

**REPORT DOCUMENTATION PAGE**

AFRL-SR-AR-TR-06-0069

Public reporting burden for this collection of information is estimated to average 1 hour per response, including the gathering and maintaining the data needed, and completing and reviewing the collection of information. Send comments regarding this collection of information, including suggestions for reducing this burden, to Washington Headquarters Services, Directorate for Information Operations and Reports, 1215 Jefferson Davis Highway, Suite 1204, Arlington, VA 22202-4302, and to the Office of Management and Budget, Paperwork Project (0142-0047).

<b>1. AGENCY USE ONLY (Leave blank)</b>		<b>2. REPORT DATE</b>	<b>3. REPORT TYPE AND DATES COVERED</b> 01 MAR 2003 - 28 FEB 2006 FINAL	
<b>4. TITLE AND SUBTITLE</b> Computer Simulations of Ion Transport across Excitable Membrane Stimulated by External Field			<b>5. FUNDING NUMBERS</b> 61102F 2301/EX	
<b>6. AUTHOR(S)</b> Dr Lin				
<b>7. PERFORMING ORGANIZATION NAME(S) AND ADDRESS(ES)</b> UNIVERSITY OF CALIFORNIA OFFICE RESEARCH ADMINISTRATION 10920 WILSHIRE BLVD #1200 LOS ANGELES CA 90024-6523			<b>8. PERFORMING ORGANIZATION REPORT NUMBER</b>	
<b>9. SPONSORING/MONITORING AGENCY NAME(S) AND ADDRESS(ES)</b> AFOSR/NE 4015 WILSON BLVD SUITE 713 ARLINGTON VA 22203			<b>10. SPONSORING/MONITORING AGENCY REPORT NUMBER</b>  F49620-03-1-0134	
<b>11. SUPPLEMENTARY NOTES</b>				
<b>12a. DISTRIBUTION AVAILABILITY STATEMENT</b> DISTRIBUTION STATEMENT A: Unlimited			<b>12b. DISTRIBUTION CODE</b>	
<b>13. ABSTRACT (Maximum 200 words)</b> This is the Final Technical Report on work performed under the support of the Air Force Office of Scientific Research (F49620-03-0134) on the subject that was changed to Terahertz radiation sources after fulfillment of its original biological direction. This report describes the motivation and approach being taken to elucidate the physical mechanism for generating radiation from DC discharge in Coaxial Resonators. The electrostatic phenomena arose in this configuration, such as plasma oscillations and sheath formation was extensively investigated by Irving Langmuir <sup>1,2</sup> . Hopefully, we will be able to study the electromagnetic effect using our particle model under development.				
<b>14. SUBJECT TERMS</b>			<b>15. NUMBER OF PAGES</b>	
			<b>16. PRICE CODE</b>	
<b>17. SECURITY CLASSIFICATION OF REPORT</b> Unclassified	<b>18. SECURITY CLASSIFICATION OF THIS PAGE</b> Unclassified	<b>19. SECURITY CLASSIFICATION OF ABSTRACT</b> Unclassified	<b>20. LIMITATION OF ABSTRACT</b> UL	

**Computer Simulations of Ion Transport across  
Excitable Membrane Stimulated by External Field**

F49620-03-1-0134

FINAL TECHNICAL REPORT

TO

AIR FORCE OFFICE OF SCIENTIFIC RESEARCH

Dr. Anthony T. Lin

Department of Physics

University of California, Los Angeles

Los Angeles, CA 90024-1547

**20060323055**

Sept. 1, 2005 to Feb. 28, 2006

## **Computer Simulations of Ion Transport across Excitable Membrane Stimulated by External Field**

This is the Final Technical Report on work performed under the support of the Air Force Office of Scientific Research (F49620-03-0134) on the subject that was changed to Terahertz radiation sources after fulfillment of its original biological direction. This report describes the motivation and approach being taken to elucidate the physical mechanism for generating radiation from DC discharge in Coaxial Resonators. The electrostatic phenomena arose in this configuration, such as plasma oscillations and sheath formation was extensively investigated by Irving Langmuir<sup>1,2</sup>. Hopefully, we will be able to study the electromagnetic effect using our particle model under development.

### I. Introduction

Terahertz radiation is loosely defined in the frequency range of 0.3 to 3 THz (wavelength range: 1000~100 $\mu$ m). Being situated between infrared light and microwave radiation, THz source is resistant to the generation and diagnostic techniques commonly employed in these well-established neighboring bands. The most significant limitation to the application of modern THz systems is the lack of high-power, low-cost, room-temperature compact THz source. One of the primary motivations for the development of THz source is its potential to extract material characteristics that are unavailable when using other frequency band. In recent years, THz spectroscopy systems have been applied to a large variety of materials both to aid the basic understanding of the material properties, and to demonstrate potential applications in sensing and diagnostics. Other applications include Terahertz tomographic imaging to replace mammography, screening passengers for explosive at airports, and broadband cell-phone communication.

Currently, there is a vast array of potential sources<sup>3</sup> each with its own advantages. Broadband THz radiation can be produced by thermal sources and, more recently, by table-top laser-driven sources using high-speed photoconductors as transient current sources for radiating antennas. Using these approaches, both attainable output power (nano to microwatt range) and efficiency ( $10^{-6}$ ) are very low. In the last decade, active research has been devoted to produce narrow band, high power (kW), and high efficiency (one percent) based on free-electron laser mechanism<sup>4</sup>. In this device, the acceleration of the electron beam (2MV) is provided by a small-size RF LINAC. The experimental set-up can be placed on a bench-top and the total area occupied is about  $1 \times 2 \text{ m}^2$ .

An alternative approach to generate THz radiation was proposed<sup>5</sup> in 1985 by Alexeff. He claimed that he obtained one watt output with  $10^{-5}$  efficiency Terahertz radiation from his table-top DC (10kV) discharge in a coaxial resonator without magnetic field (Fig.1). However, the physical mechanism responsible for generating the THz radiation in this configuration still remains controversially. There are the following three

as it transverses the sheath region around the anode wire<sup>7</sup>. In microwave range, the performance based on DC discharge is unable to compete against the conventional devices in output power and efficiency. However, most experimental results published were in this region. In order to be able to validate simulation results, simulations will be carried out in GHz range first to isolate the physical mechanism. The parameters will then be scaled up to simulate THz generation.

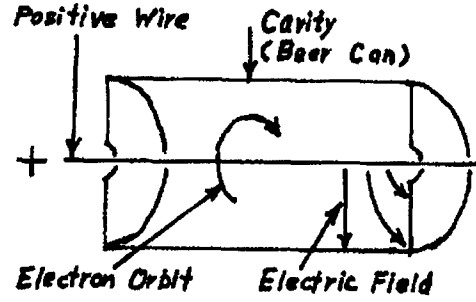


Fig. 1. Original Maser Design

## II. Review of Experimental Results

Three experimental results that are relevant to the electromagnetic radiation generation based on the concentric cylindrical diode configuration will be reviewed here. A DC discharge across a diode can be pure electron discharge or discharge in gases.

### 1. Orbitron

The basic principle of operation of an orbitron<sup>8</sup> is believed to be that electrons oscillate (orbital motion) in a system in which the electrons both are confined for a long time and the oscillation frequency varies with energy. When an electron interaction with the cavity mode of the surrounding metal container to give energy to the cavity EM field, it will slow down and then move closer to the center conductor since the electrostatic field force will be greater than the centrifugal force. The electron will then have a slightly smaller equilibrium radius and corresponding higher angular velocity. It can now further interact with the cavity EM field in approximate synchronism with it and this process may continue until the electron is intercepted by the center conductor. By balancing the centrifugal force and the electrostatic force in a coaxial system, we have.

$$\frac{mv^2}{r} = -eE_r = -\frac{eV_0}{r \ln\left(\frac{r_1}{r_0}\right)}, \quad (1)$$

where  $r_1$  is the radius of the cavity and  $r_0$  is the radius of the wire. The electron orbital frequency is given by

$$f = \frac{\omega_0}{2\pi} = \frac{v}{2\pi r} = -\frac{eV_0}{2\pi r m \ln\left(\frac{r_1}{r_0}\right)}. \quad (2)$$

From Eq.(2), the highest frequency that can be obtained is when  $r = r_0$ . The original orbitron design is shown in Figure 1. By using the following parameters:  $r_0 = 8.5 \times 10^{-6}$  m,  $V_0 = 10$  kV, and  $P(\text{gas pressure}) = 2 \times 10^{-2}$  mm, the resulting current is 20A and device output power is about 1 watt (eff. =  $10^{-5}$ ) at 1 THz.

Using  $r_1 = 5 \times 10^{-3}$  m, the highest frequency becomes  $f_0 = 6.5 \times 10^{11}$  Hz. On the other hand, the plasma frequency for a fully ionized background gas is about  $2.7 \times 10^{11}$  Hz. The fourth harmonic of plasma oscillation can also reach 1 THz. In a later experiment<sup>8</sup>, the wire radius is increased to  $2.5 \times 10^{-5}$  m and the applied voltage is reduced to 500V. In doing so, the current drops to only a few mA and the orbitron emits a surprisingly stable line spectrum of a few GHz, as shown in Fig. 2. The observed lowest frequency mode is believed to be due to coupling to the external circuit. The discharge current is observed to affect the output frequency. However, experimental results do not provide any conclusive evidence that the physical mechanism for radiation generation is due to electron orbital motion around the positively charged wire.

## 2. Diverging Concentric Diodes

The theoretical effort to produce negative impedance by means of an electron discharge in a plane diode<sup>9</sup> has been known since 1928. The negative resistance appears whenever the electron transit time between electrodes is approximately  $1\frac{1}{4}$ ,  $2\frac{1}{4}$ ,  $3\frac{1}{4}$  etc cycles of a given high-frequency current. This concept was applied to a cylindrical configuration<sup>10</sup> (Fig. 3a) in which the inner conductor is the emitter (cathode) while the outer conductor is the collector (anode) that is biased positively. Since the negative resistance is low, it is essential to use a nearly closed structures to reduce the losses caused by radiation of energy. For the production of EM oscillations, the capacitance of the diode must be combined with a resonant structure having the proper inductance to resonate at the desired frequency, and having a resistance which effectively is less in magnitude than that of the electron beam. Because of the low losses thus required of the device operation the properties of concentric lines and of tuned

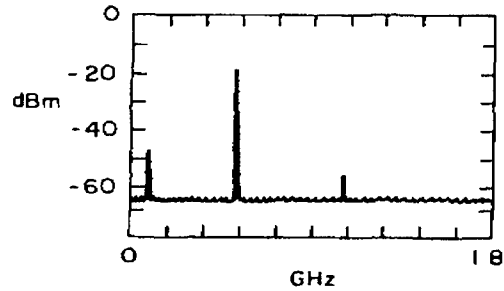


Fig. 2. Spectrum of gas filled steady static Orbitron.

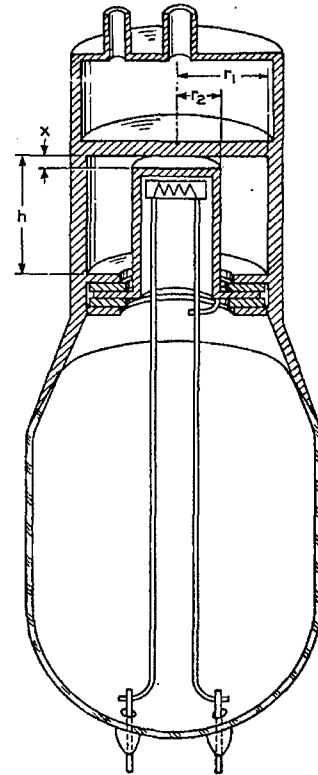


Fig. 3a Ten-centimeter diode used in tests.

Diode	$r_1$	$r_2$	$x$	$h$
No. 24	1.270	0.635	0.203	1.870
No. 37	1.220	0.635	0.105	1.870

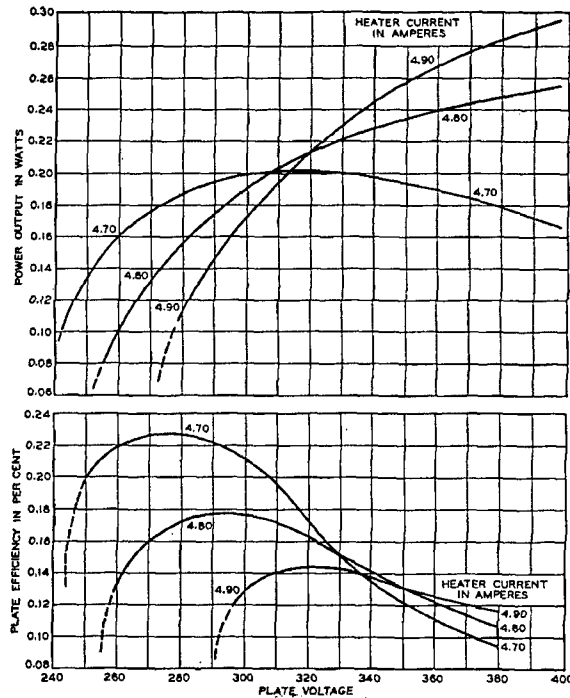


Fig. 3b. Power output and plate efficiency for diode no. 24.

copious harmonics was detected. In this experiment<sup>7</sup>, the small electrode acts as an rf antenna. A typical discharge can be divided into plasma region with equal electron and ion densities and an electron-rich plasma sheath. The sheath-plasma resonance is a well-known phenomenon of rf probes and antennas in plasmas. Basically, an electron-rich sheath acts like a capacitor (diode) while a field-free cold plasma can behave inductively ( $\epsilon = 1 - \frac{\omega_p^2}{\omega^2} < 0$  for  $\omega < \omega_p$ ) such that a resonance is possible. The instability is driven by a negative rf sheath resistance associated with the electron inertia effect in the diode like electron-rich sheath. The maximum values which the negative resistance attains occur in the neighborhood of transit angles given by

$$\theta = \omega\tau = 2\pi n + \frac{\pi}{2}, \quad n=1,2,3,\dots \quad (3)$$

where  $\tau$  is the electron transit time as it streams through the sheath region.

Using a second movable floating rf probe, the field amplitude has been mapped versus radial distance from the exciter probe (Fig. 4a). It shows that both the fundamental and the second harmonic exhibit a monotonic amplitude decay in the near-zone. With increasing distance ( $r > \frac{c}{\omega_p} \simeq 1.6$  cm) the fundamental amplitude truly vanishes while the harmonic remains observable throughout the plasma and beyond. The result clearly indicates a highly localized field pattern of the nonradiating fundamental mode and a broader pattern of the propagating second harmonic. This also confirms that

cavities offer a favorable method of approach. The experiment was carried out using  $V_0 = 300V$  and  $I = 500mA$ . (no gas pressure was given). Power output and efficiency data obtained during the experiment are shown in Fig. 3b. Power output of a few tenths of a watt at efficiency of tenths of a percent are achieved. Again, there is no convincing evidence from this experiment that identifies the physical mechanism for producing the EM radiation.

### 3. Microwave Radiation From Electron-Rich Sheath-Plasma Resonance

By placing a small size electrode (with a positive dc bias), which can be a plane disc, sphere, or cylinder, into large size afterglow plasma, microwave radiation with

the plasma behaves inductively ( $\omega < \omega_p$ ). The observed field polarization observed (ref. 7) is inconsistent with other radiation mechanism proposed for earlier observations of EM emissions from positively biased wires in plasmas such as beam-plasma instability<sup>6</sup> and orbitron mechanism<sup>5</sup>. The most direct confirmation that the above-mentioned instability mechanisms are unable to explain the present observation is shown in Fig. 4b. EM harmonic lines are observed for all basic electrode geometries: plane, spherical, and cylindrical. It is inconceivable that long-lived electron orbitron or counterstreaming electron beams arise at a large plane electrode, whereas sheath-plasma instabilities can occur for any electrode geometry. The observed instability exhibits threshold, growth, and saturation. The rf voltage and power saturate at levels small compared to the dc voltage and power, respectively. The conversion efficiency is about  $5 \times 10^{-5}$ . This low efficiency may be attributed to that the small size antenna radiates into large volume plasma and the lack of resonator to confine the EM radiation.

### III. Numerical Model

The efficiency of Terahertz sources based on the DC discharge in coaxial resonator may be substantially improved from  $10^{-5}$  provided that the generation mechanism can be identified. In order to fulfill this goal, the best approach is to build a particle code that includes electrostatic and electromagnetic interactions as well as the DC discharge physics. Since the electrostatic field plays a very important role in determining the electron equilibrium orbit, we will start with building an electrostatic particle code bounded by coaxial resonator. The B-spline of fourth order (degree 3) is used for solving the two dimensional Poisson equation in cylindrical coordinates

$$\frac{\partial^2 \Phi}{\partial r^2} + \frac{1}{r} \frac{\partial \Phi}{\partial r} + \frac{\partial^2 \Phi}{\partial z^2} = -4\pi\rho, \quad (4)$$

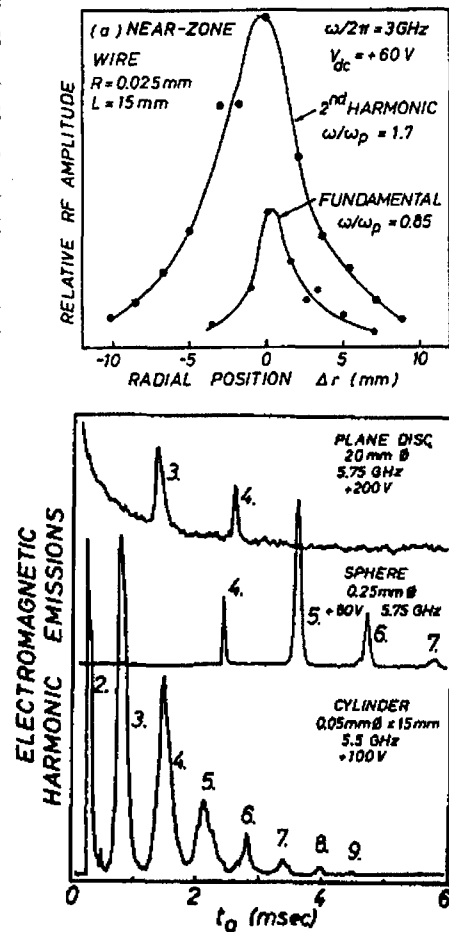


Fig. 4. (a) Radial rf amplitude profile showing a broader half-width for the propagating harmonics than for the evanescent fundamental emission. (b) Comparison of emission spectra for different electrode geometries showing the existence of the sheath-plasma instability for all shapes and ruling out the orbital instability mechanism.

with the boundary conditions of  $\Phi(r,0) = \Phi(r,L) = \Phi(r_w,z) = 0$ . Expand the functions  $\Phi$  and  $\rho$  along the  $z$ -direction in terms of sine functions

$$\Phi = \sum_{k=1}^{N_z} \Phi_k(r) \sin \frac{k\pi}{L} z, \quad \rho = \sum_{k=1}^{N_z} \rho_k(r) \sin \frac{k\pi}{L} z, \quad (5)$$

where  $N_z$  is the number of grid points in the  $z$ -direction. Substituting (5) into (4) yields

$$\Phi_k'' + \frac{1}{r} \Phi_k' - \left(\frac{k\pi}{L}\right)^2 \Phi_k = -4\pi\rho_k, \quad (6)$$

A spline can be expressed in the following form

$$S(r) = \sum_{i=1}^n a_i B_i(r) = \Phi_k(r), \quad (7)$$

where  $n = N_r + 2$  ( $N_r$  is the number of grid points in the radial direction).

The detailed property of B-spline has been described in Ref. [11]. In a coaxial resonator, additional boundary conditions at the center conductor  $\Phi(r_0,z) = V_0$  must be imposed. With this applied potential, the resulting surface charge on the inner conductor is

$$\sigma = \frac{-V_0}{4\pi r_0 \ln\left(\frac{r_1}{r_0}\right)} \text{ and the radial electric field is}$$

$$E_r(r_0) = -\frac{V_0}{r_0 \ln\left(\frac{r_1}{r_0}\right)} = -\sum_{i=1}^n a_i B_i'(r_0). \quad (8)$$

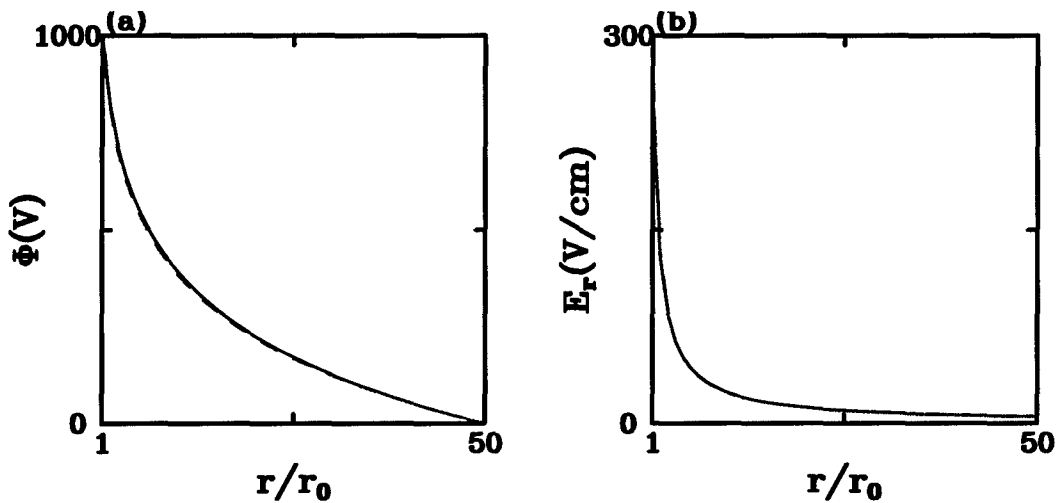


Fig. 5 Comparison of (a) potential and (b) radial electric field profiles between theoretical results (dark curves) and that from the B-spline calculations (dashed red curves).

For the case of infinite coaxial cylinders, the theoretical profile of

$$E_r(r) = \frac{V_0}{r} \frac{1}{\ln(\frac{r_1}{r_0})} \quad \text{and} \quad V(r) = V_0 \frac{\ln(\frac{r}{r_0})}{\ln(\frac{r_1}{r_0})}, \quad (9)$$

are displayed as black curves in Fig. 5. To test the accuracy of the B-spline approach, results from the B-spline solution are shown as red curves in the same figure. The potential contour obtained from the B-spline solution for the case of  $\rho = 0$  in a two dimensional system ( $r, z$ ) is shown in Fig. 6.

Since the maximum energy an electron can attain is in the neighborhood of 10 kV, the relativistic equation of motion employed in our particle code for simulating microwave devices is simplified to become non-relativistic. In order to allow all possible mechanisms to occur, three dimensional electron orbital motions will be allowed. The electron equilibrium orbit can be derived from the Lagrangian of the energy equation

$$\frac{m}{2} \left[ \left( \frac{dr}{dt} \right)^2 + r^2 \left( \frac{d\theta}{dt} \right)^2 \right] = eV(r). \quad (10)$$

The cross-sectional view of four representative electron orbits starts with different initial condition is shown in Fig. 7. Here electrons start with the same kinetic energy that is equal to the potential energy at the initial position but at different angle  $\psi$  with respect to the radius vector.

The electromagnetic field can be taken into account by using the same technique as we have employed in simulating microwave devices<sup>11</sup>. The scalar function appropriate to the lowest E-mode in a coaxial guide is  $C_{00} = \ln r / \sqrt{2\pi \ln \frac{r_1}{r_0}}$ . Hence the field components of this mode are

$$E_r = E_t(z) \frac{1}{r \sqrt{2\pi \ln \frac{r_1}{r_0}}}$$

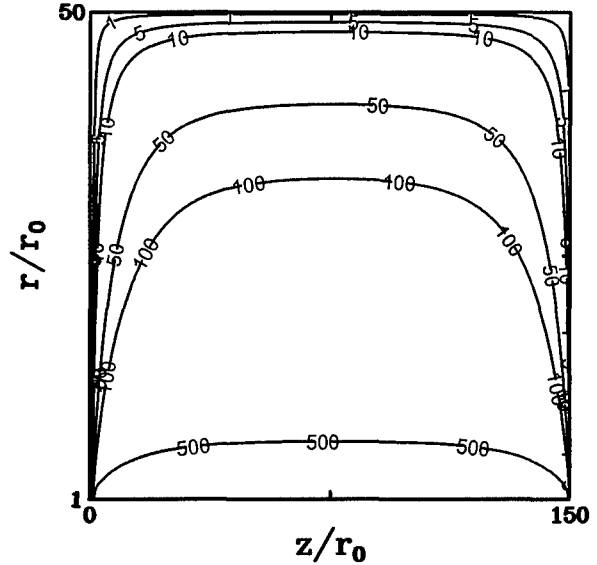


Fig. 6 Two dimensional ( $r, z$ ) potential contour calculated from the B-spline solution.

$$B_\phi = B_t(z) \frac{1}{r \sqrt{2\pi \ln \frac{r_1}{r_0}}} \quad (11)$$

$$E_\phi = E_z = H_r = H_z = 0$$

and the corresponding Maxwell's equations are

$$\frac{\partial E_r}{\partial t} = c \left( -\frac{\partial B_\phi}{\partial z} \right) - 4\pi J_r \quad (12)$$

$$\frac{\partial B_\phi}{\partial t} = -c \left( \frac{\partial E_r}{\partial z} \right),$$

where  $E_t(z)$  and  $B_t(z)$  can be expanded by using Cosine and Sine functions respectively to satisfy their boundary conditions. This transverse electromagnetic mode is the dominant or principal mode in coaxial guide. If the higher E-modes are needed, they can be derived from the scalar functions  $C_i = Z_m \left( \chi_i \frac{r}{r_0} \right) \cos m\theta$  and be included by keeping only a few  $m$  modes.

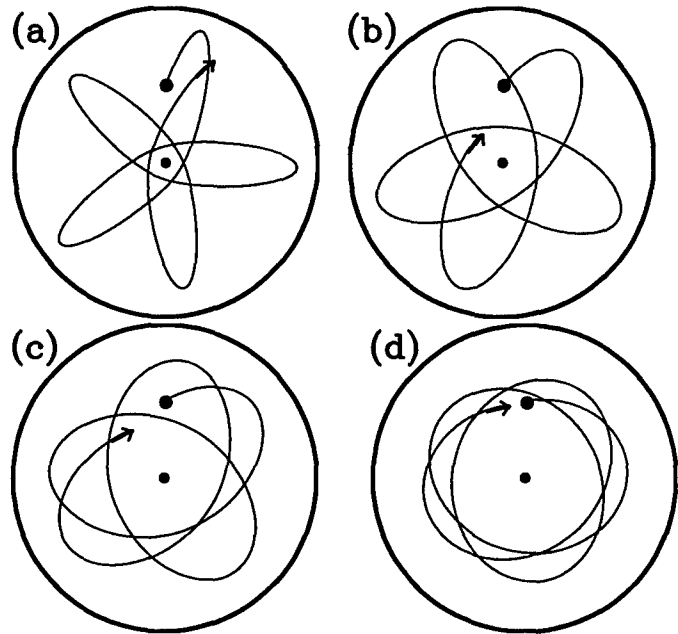


Fig. 7 Example of electron orbits in a logarithmic potential from particle simulations,  $\psi =$  (a)  $20^\circ$ , (b)  $40^\circ$ , (c)  $60^\circ$ , (d)  $80^\circ$ .

## References

1. L. Tonks and I. Langmuir, "Oscillations In Ionized Gases," *Phys. Rev.* 33, 195(1929).
2. I. Langmuir and K. T. Compton, "Electrical Discharge In Gases-Part II. Fundamental Phenomena In Electrical Discharges," *Rev. of Modern Phys.* 3, 191(1931).
3. P. H. Siegel, "Terahertz Technology," *IEEE Trans. Microwave Theory Techn.*, MTT-50, 910(2002).
4. A. Doria, et.al, "Enhanced Coherent Emission of Terahertz Radiation by Energy-Phase Correction in a bBunched Electron Beam, *Phys. Rev. Lett.*, 93, 264801-1(2004).
5. I. Alexeff, F. Dyer, and W. Nakoneczny, "Orbitron Operation At 1 Thz," *Int. J. of Infrared and Millimeter Waves*, 6, 481(1985).
6. R. W. Schumacher and R. J. Harvey, *Bull. Amer. Phys. Soc.*, 29, 1179(1984).
7. R. L. Stenzel, "Instability of the Sheath-Plasma Resonance," *Phys. Rev. Lett.*, 60, 704(1988).
8. I. Alexeff, F. Dyer, and M. Radar, "Recent Results On the Orbitron Maser," *Nul. Inst. And Methods in Phys. Res.*, A285, 228(1989).
9. W. E. Benham, "Theory of the Internal Action of Thermionic Systems at Moderately High Frequencies," *Phil. Mag.*, 11, 457(1931).
10. F. F. Levwellyn and A. E. Bowen, "The Production of Ultra-High-Frequency Oscillations by Means of Diodes," *Bell System Technical Journal*, 18, 280(1939).
11. C. C. Lin and A. T. Lin, "A New Algorithm for Solving Maxwell's Equations in High-Power Microwave Device Simulations," *IEEE Trans. On Plasma Science*, 26, 893(1998).